ON MULTIPLE SPIN RESONANCES FOR THE POLARIZED PROTON†

S. TEPIKIAN, S. Y. LEE, and E. D. COURANT

Brookhaven National Laboratory, Upton, New York 11973

We reformulate the acceleration of polarized protons through a spin resonance in terms of the spin transfer matrix. The method is then applied to the acceleration of polarized protons through nonoverlapping spin resonances. We find that the phase factor between two resonances is important when two resonances have moderate strength. The method has also been applied to resonance jumping. Good agreement with the AGS experiment is achieved. However, when two resonances overlap, no analytic solution is available; we therefore resort to a numerical calculation by solving the system of first-order differential equations. We find that: (i) overlapping resonances can be considered as a single resonance with an effective strength that oscillates rapidly as a function of the spacing of these resonances. Because of this rapid fluctuation, tune spread averaging is also considered. (ii) For isolated resonances, the final spin also oscillates rapidly around a nominal value, which depends solely on the Froissart–Stora equation of individual resonance. Our analytic results in both cases agree very well with the numerical solutions.

1. INTRODUCTION

The scattering of polarized protons is one of the important tools for studying the nature of fundamental interactions.[1] Their acceleration has been discussed extensively in the past few years,[2–8] and great understanding has been achieved theoretically and experimentally. Unfortunately most investigative methods are limited only to a single resonance and cannot be extended easily to the case of many resonances. Since high-energy polarized proton experiments are of great interest,[1] the acceleration of polarized proton beams through *many* depolarizing resonances is also important in accelerator physics.

Two or more depolarizing resonances can be classified into two cases: (1) nonoverlapping resonances, where each spin particle is under the influence of a single resonance at a time; and (2) overlapping resonances. In the first situation, the spin equation for a single resonance can be solved analytically. Accordingly, in this paper, we develop a transfer matrix method for the spin particle. Particle acceleration through several nonoverlapping resonances can be handled via matrix products. On the other hand, when resonances are overlapping (e.g., the 60-ν intrinsic resonance and the 51 imperfection resonance at Brookhaven's AGS), there is no known analytic solution. Therefore, we will solve the differential equation numerically and then analyze the result analytically.

The plan of this paper is as follows: In Section 2, a spin transfer matrix method is developed.[9] The method is then applied in Section 3 to study the physics of the spin resonance tune jump and to study the effects of resonances on the spin after passing through two nearby, yet nonoverlapping, spin resonances. For the case of two overlapping resonances, we resort in Section 4 to the numerical ordinary differential equation solver (DEABM).[10] Section 5 discusses the effect of the tune spread averaging, and our conclusions are summarized in Section 6.

2. SPIN TRANSFER MATRIX

Spin precession for a group of particles in a magnetic field is described by the Bargman, Michel, and Telegdi equation for a single classical particle,[2]

$$\frac{d\mathbf{S}}{dt} = \frac{e}{\gamma mc} \mathbf{S} \times \left[(1 + \gamma G)\mathbf{B}_\perp + (1 + G)\mathbf{B}_\parallel - \left(1 + \gamma G - \frac{1}{1+\gamma} \right) \frac{\mathbf{v}}{c} \times \mathbf{E} \right] \quad (1)$$

where $G = (g - 2)/2$ is the Pauli anomalous magnetic g factor; $\mathbf{S}$ is the average spin of the group of particles in the particle rest frame; $\mathbf{B}_\perp$ and $\mathbf{B}_\parallel$ are magnetic fields transverse and parallel, respectively, to the velocity $\mathbf{v}$ of the particles; $\mathbf{E}$ is the electric field; and γ, e, m, c, and t are, respectively, the Lorentz factor, electric charge, mass, speed of light, and time in the laboratory frame.

Assuming that the beam particles travel along a nominal path, Froissart and Stora[3] and Courant and Ruth[4] have derived an equation for the spin precession in circular accelerators (see also Appendix A):

$$\frac{d\mathbf{S}}{d\theta} = \mathbf{S} \times \mathbf{\Omega} \quad (2)$$

$$\mathbf{\Omega} = -t\hat{x} + r\hat{s} - \kappa\hat{y}, \quad (3)$$

where $\kappa = \gamma G$ is the spin precession frequency in the guide field, $r = (1 + \gamma G)y' - \rho(1 + G)(y/\rho)'$, and $t = (1 + \gamma G)\rho y''$; ρ is the radius of curvature of the dipoles, and the prime stands for d/ds (the derivative with respect to the path length of the particles).

Using a two-component spinor ψ, we can also define the spin as

$$\mathbf{S} = \psi^\dagger \boldsymbol{\sigma} \psi. \quad (4)$$

Thus,

$$\frac{d\mathbf{S}}{d\theta} = \frac{d\psi^\dagger}{d\theta} \boldsymbol{\sigma} \psi + \psi^\dagger \boldsymbol{\sigma} \frac{d\psi}{d\theta} = \frac{i}{2} \psi^\dagger (\boldsymbol{\sigma}, H)\psi, \quad (5)$$

where we have assumed that the spinor satisfies the spinor Hamiltonian equation,

$$\frac{d\psi}{d\theta} = \frac{i}{2} H\psi, \quad (6)$$

where H is Hermitian.

Equating Eqs. (6) and (2), we obtain

$$\frac{d\psi}{d\theta} = -\frac{i}{2}\begin{pmatrix} G\gamma(\theta) & -\zeta \\ -\zeta^* & -G\gamma(\theta) \end{pmatrix}\psi, \tag{7}$$

where $\zeta = -t - ir$ is the depolarizing resonance strength and θ is the angle around the accelerator, i.e.,

$$\theta = \int_0^s \frac{ds}{\rho(s)}, \tag{8}$$

where s is the distance traveled by the particle and $\rho(s)$ is the radius of curvature of its path. The off-diagonal component of the matrix in Eq. (7), ζ, causes the spin to precess away from the vertical and may lead to depolarization. Due to the periodic nature of the circular accelerator, ζ can be expanded into an almost-periodic Fourier series,

$$\zeta = \sum_l \varepsilon_l e^{-i\chi_l(\theta)}, \tag{9}$$

where ε_l is the resonance strength, which depends mainly on the horizontal focusing and defocusing magnetic field.[4] A stronger-focusing accelerator tends to increase the resonance strength.

A circular accelerator has a periodicity of 2π (one revolution) and also a betatron tune periodicity. Therefore, the Fourier component $\chi_l(\theta)$ can be expressed as

$$\chi_l(\theta) = K_l \cdot \theta, \tag{10}$$

with

$$K_l = \begin{cases} k & \text{imperfection resonance} \\ kP \pm \nu(\theta) & \text{intrinsic resonance} \\ k \pm \nu(\theta) & \text{gradient-error resonance,} \end{cases} \tag{11}$$

where k, P and $\nu(\theta)$, are an integer, the periodicity of the machine, and the vertical tune of the machine, respectively. In the normal operation of the accelerator, the machine tune $\nu(\theta)$ is a constant. However, when a tune jump is applied to the accelerator, the machine tune ν will depend on time or θ. In a perfect accelerator, there are no imperfection or gradient-error resonances. In an actual machine, these can be reduced by quality control and correction elements. Intrinsic resonances must, however, be treated differently. The standard approach is called resonance jumping.[4,6-8]

We consider only a single resonance in this section. (This procedure is justified for situations in which the resonances are well-separated; the calculation for resonances overlapping each other is discussed in Section 4.) We shall assume further that the acceleration of the particle is a continuous linear function, i.e.,

$$\gamma G = K_0 + \alpha\theta, \tag{12}$$

where K_0 can be chosen to be the resonance position at $\theta = 0$. Making the transformation to the intrinsic precession frames (interaction picture), i.e.,

$$\psi(\theta) = \exp\left(-\frac{i}{2}\int_0^\theta \gamma G \, d\theta \sigma_3\right)\Phi(\theta), \tag{13}$$

where σ_3 is the third component of the Pauli matrix, we obtain

$$\frac{d}{d\theta}\Phi(\theta) = +\frac{i}{2}$$

$$\begin{pmatrix} 0 & \varepsilon \exp\frac{i}{2}\{[(K_0 - K)\theta + \frac{1}{2}\alpha\theta^2]\} \\ \varepsilon^* \exp\left\{-\frac{i}{2}[(K_0 - K)\theta + \frac{1}{2}\alpha\theta^2]\right\} & 0 \end{pmatrix}\Phi(\theta). \quad (14)$$

The resonance effect is greatest when the exponent in Eq. (14) reaches a stationary phase, i.e.,

$$d/d\theta(-K\theta + K_0\theta + \frac{1}{2}\alpha\theta^2)|_{\theta=\theta_R} = 0.$$

At the resonance, θ_R, the perturbing kicks add up coherently from turn to turn. We choose $K_0 - K = 0$, so that $\theta_R = 0$ corresponds to the resonance position. Expressing the spinor wave functions in terms of two components $\xi_1(\theta)$ and $\xi_2(\theta)$, i.e.,

$$\Phi(\theta) = \begin{pmatrix} \xi_1(\theta) \\ \xi_2(\theta) \end{pmatrix},$$

we have then

$$\frac{d}{d\theta}\xi_1(\theta) = +\frac{i}{2}\varepsilon e^{(i/2)\alpha\theta^2}\xi_2(\theta), \quad (15a)$$

$$\frac{d}{d\theta}\xi_2(\theta) = +\frac{i}{2}\varepsilon^* e^{-(i/2)\alpha\theta^2}\xi_1(\theta). \quad (15b)$$

Eliminating $\xi_2(\theta)$ in Eqs. (15a) and (15b) gives a second-order differential equation in $\xi_1(\theta)$:

$$\frac{d^2}{d\theta^2}\xi_1(\theta) - i\alpha\theta\frac{d}{d\theta}\xi_1(\theta) + \frac{|\varepsilon|^2}{4}\xi_1(\theta) = 0. \quad (16)$$

The solution of this equation can be expressed as

$$\xi_1(\theta) = Az(\theta) - Bw(\theta), \quad (17)$$

where z and w are given in terms of confluent hypergeometric functions.[11,12]

$$z(\theta) = M\left(iq, \frac{1}{2}; \frac{i}{2}\alpha\theta^2\right), \quad (18a)$$

$$w(\theta) = +\frac{i}{2}\varepsilon\theta e^{(i/2)\alpha\theta^2}M\left(1 - iq, \frac{3}{2}; -\frac{i}{2}\alpha\theta^2\right) \quad (18b)$$

where the dimensionless resonance strength q is given by

$$q = \frac{|\varepsilon|^2}{8\alpha}.$$

From Eq. (15a) one finds

$$\xi_2(\theta) = A\bar{w}(\theta) + B\bar{z}(\theta), \quad (19)$$

where $\bar{z}(\theta)$ and $\bar{w}(\theta)$ are complex conjugate functions of $z(\theta)$ and $w(\theta)$, respectively. From Eqs. (17) and (19), we write

$$\Phi(\theta) = \begin{pmatrix} z(\theta) & -w(\theta) \\ \bar{w}(\theta) & \bar{z}(\theta) \end{pmatrix} \begin{pmatrix} A \\ B \end{pmatrix}$$

$$= T(\theta) \begin{pmatrix} A \\ B \end{pmatrix}. \tag{20}$$

Equation (20) defines the matrix $T(\theta)$, which has the property that

$$\det[T(\theta)] = 1. \tag{21}$$

This can be verified easily from the spinor equation [Eq. (16)] due to the conservation of the magnitude of the spin in the course of acceleration. Constants A and B are determined from the initial conditions as

$$\begin{pmatrix} A \\ B \end{pmatrix} = T^{-1}(\theta_i)\Phi(\theta_i). \tag{22}$$

Equation (20) thus becomes

$$\Phi(\theta) = T(\theta)T^{-1}(\theta_i)\Phi(\theta_i). \tag{23}$$

Here $T(\theta)T^{-1}(\theta_i)$ is called the spin transfer matrix. It allows us to transform the spinor wave function from one side to the other side of a resonance. The essential idea is similar to the wave propagation matrix method in the semiclassical theory[13] or the transfer matrix method in the lattice calculation.[14] Ruth has given a similar formulation by using perturbation series expansion.[15] However, his approach cannot easily be generalized.

Using the asymptotic expansion of the confluent hypergeometric functions of Eqs. (18) for large $\frac{1}{2}\alpha\theta^2$, we obtain the asymptotic spin transfer matrix as (see Appendix B)

$$T(\theta)T^{-1}(\theta_i) = \exp\left[-iq\ln\left(\tfrac{1}{2}\alpha\,|\theta|^2\right)\sigma_3\right]U(q)\exp\left[+iq\ln\left(\tfrac{1}{2}\alpha\,|\theta_i|^2\right)\sigma_3\right], \tag{24}$$

where

$$U(q) = \begin{pmatrix} e^{-2\pi q} & C(q) \\ -\bar{C}(q) & e^{-2\pi q} \end{pmatrix} \tag{25}$$

with

$$C(q) = -\frac{i}{4}\,\varepsilon\,\sqrt{\frac{2}{\alpha}}\,\frac{\Gamma(\frac{1}{2}+iq)}{\Gamma(1-iq)}\,e^{i\pi/4}e^{-\pi q}(e^{\pi q}+e^{-\pi q}).$$

This expansion is valid, provided that the asymptotic condition

$$|\theta| \quad \text{and} \quad |\theta_i| \gg \theta_A \tag{26a}$$

is satisfied, where (See Appendix B)

$$\tfrac{1}{2}\alpha\theta_A^2 \gg q\,\frac{\cosh\pi q}{\sinh\pi q} \tag{26b}$$

and

$$\frac{1}{2}\frac{\tfrac{1}{2}\alpha\theta_A^2}{\ln\left(\tfrac{1}{2}\alpha\theta_A^2\right)} \gg q \tag{26c}$$
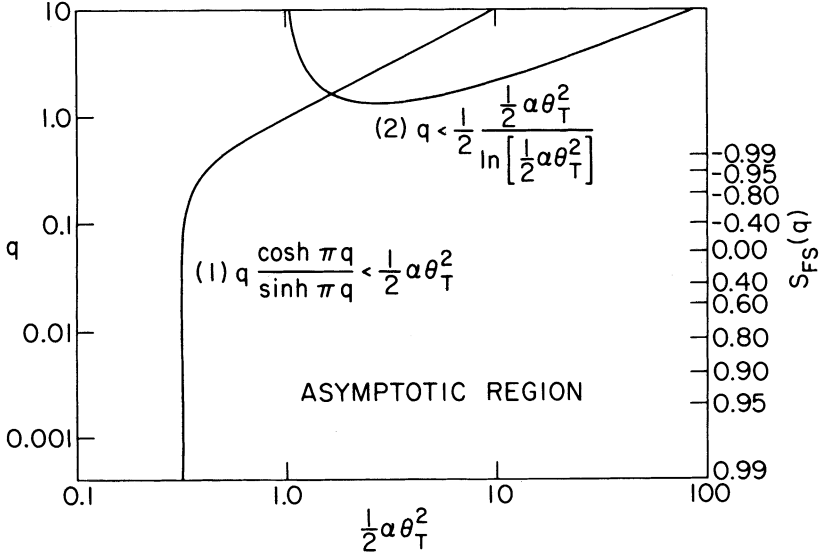
FIGURE 1   Plot of the dimensionless resonance strength q as a function of $\frac{1}{2}\alpha\theta_T^2$ for the asymptotic conditions (Eqs. B-7 and B-9). The corresponding Froissart–Stora value of polarization is also shown.

and q is the dimensionless resonance strength defined earlier. Equation (26b) shows that the spinor wave function is dominated by the first term of the asymptotic expansion. When Eq. (26c) is also considered, the precession frequency modulation due to the spin resonance [Eq. (24)] would be much smaller than the normal spin precession frequency. Figure 1 shows the curves for the conditions of Eqs. (26). We expect that θ_A should be an order of magnitude greater than θ_T obtained from Fig. 1, to obtain a good asymptotic region. As an example, the $K = \nu$ resonance of the AGS at Brookhaven is $|\varepsilon| = 0.00786$. The asymptotic region is estimated to be $|\gamma G - K| \gg 0.02$.

For a single resonance, our matrix equation [Eq. (25)] gives trivially the Froissart–Stora formula,[3] i.e.,

$$S_{FS}(q) = 2e^{-4\pi q} - 1 \tag{27}$$

for an initial $\begin{pmatrix} 1 \\ 0 \end{pmatrix}$ spinor wave function. Since spin resonances outside the asymptotic regions give a negligible effect to the spin of the particles (except the modulating phases), the spin transfer matrix can be applied successively through each resonance to calculate the effect on the total spin. This topic will be discussed in the next section. We note especially that, when the resonances are moderately strong, the modulating phase becomes very important also.

3. APPLICATION OF THE SPIN TRANSFER MATRIX

3.1. Two Non-overlapping Resonances

Let us consider the acceleration of the particles through two resonances, where $\zeta(\theta)$ is given by

$$\zeta(\theta) = \varepsilon_1 e^{i\kappa_1\theta} + \varepsilon_2 e^{i\kappa_2\theta}. \tag{28}$$

The resonance tunes κ_1 and κ_2 are well outside the asymptotic region of one another (nonoverlapping). We can therefore solve the spinor wave function for each resonance separately and match the wave functions. Let θ_1 and θ_2 represent the angles for which the particle crosses the resonances κ_1 and κ_2, respectively; i.e.,

$$\kappa_1 = G\gamma(\theta_1), \tag{29a}$$

$$\kappa_2 = G\gamma(\theta_2). \tag{29b}$$

We can choose an angle θ_M in the asymptotic region of both resonances such that

$$\theta_1 \ll \theta_M \ll \theta_2. \tag{30}$$

Using the spin transfer matrix of Eq. (23) twice, we obtain the spinor wave function passing through two resonances as

$$\Phi(\theta - \theta_2) = T_2(\theta - \theta_2)T_2^{-1}(\theta_M - \theta_2)$$

$$\times \exp\left[+\frac{i}{2}\int_{\theta_1}^{\theta_2}\gamma G\,d\theta\sigma_3\right]T_1(\theta_M - \theta_1)T_1^{-1}(\theta_{\text{inj}} - \theta_1)\Phi(\theta_{\text{inj}} - \theta_1) \tag{31}$$

where θ_{inj} and θ are the injection and observation angles, respectively. The spin transfer matrices $T_1 T_1^{-1}$ and $T_2 T_2^{-1}$ depend on resonances ε_1 and ε_2, respectively. The phase factor between the spin transfer matrices comes from matching the wave function in the laboratory frame. If the asymptotic condition discussed in Appendix A holds for θ, θ_M, and θ_{inj}, we have

$$\Phi(\theta - \theta_2) = \exp\left\{-iq_2\ln\left[\tfrac{1}{2}\alpha(\theta - \theta_2)^2\right]\sigma_3\right\}$$

$$\cdot U(q_2)\exp\left(i\{q_2\ln\left[\tfrac{1}{2}\alpha(\theta_M - \theta_2)^2\right]\right.$$

$$\left. - q_1\ln\left[\tfrac{1}{2}\alpha(\theta_M - \theta_1)^2\right] - \tfrac{1}{2}\int_{\theta_1}^{\theta_2}\gamma G\,d\theta\}\sigma_3\right) \tag{32}$$

$$\cdot U(q_1)\exp\left\{+iq_1\ln\left[\tfrac{1}{2}\alpha(\theta_{\text{inj}} - \theta_1)^2\right]\sigma_3\right\}\Phi(\theta_{\text{inj}} - \theta_1),$$

where the phase factors in front of $U(q_2)$ and behind $U(q_1)$ are diagonal in the spinor space and therefore irrelevant to the final spin. When the asymptotic condition of Eq. (26c) is also considered, the phase modulation due to the resonances can be neglected; therefore, Eq. (32) becomes

$$\Phi(\theta_f) = U(q_2)\exp\left(-\frac{i}{2}\int_{\theta_1}^{\theta_2}\gamma G\,d\theta\sigma_3\right)U(q_1)\Phi(\theta_i), \tag{33}$$

where

$$q_2 = |\varepsilon_2|^2/8\alpha., $$
$$q_1 = |\varepsilon_1|^2/8\alpha \tag{34}$$

are the dimensionless resonance strengths of the two resonances. Particle rotating angles in a circular accelerator, θ_1 and θ_2, correspond to the resonance condition of Eqs. (29). Note that we have neglected the slow precession phase due to resonances in Eq. (33).

The phase factor in Eq. (33) can be expressed as

$$f = \tfrac{1}{2} \int_{\theta_1}^{\theta_2} \gamma G \, d\theta' = \frac{1}{4\alpha} (\kappa_2^2 - \kappa_1^2). \tag{35}$$

Let us assume a full spin-up polarization for the initial state, i.e., $\Phi(\theta_i) = \begin{pmatrix} 1 \\ 0 \end{pmatrix}$. With $U(q)$ as defined in Eq. (25), the final polarization S of $\Phi(\theta_f)$ in Eq. (33) can be obtained easily as

$$S = S_N(q_2, q_1) + S_F(q_2, q_1) \cos \chi, \tag{36}$$

where

$$S_N(q_2, q_1) = S_{FS}(q_2) S_{FS}(q_1), \tag{37}$$

$$S_F(q_2, q_1) = \{[1 - S_{FS}^2(q_2)][1 - S_{FS}^2(q_1)]\}^{\frac{1}{2}}, \tag{38}$$

$$\chi = 2f + \mu_1 - \mu_2 + \pi \tag{39}$$

with

$$\mu_i = \arg \frac{\Gamma(\tfrac{1}{2} + iq_i)}{\Gamma(1 - iq_i)}, \tag{40}$$

$$S_{FS}(q_i) = 2e^{-4\pi q_i} - 1. \tag{41}$$

Equation (36) consists of two parts: (i) a Δ-parameter-independent part $S_N(q_2, q_1)$, which is equal to the product of the Froissart–Stora values of each resonance in Eq. (41) and (ii) an oscillatory part with amplitude $S_F(q_2, q_1)$. When the spacing $\Delta = \kappa_2 - \kappa_1$ changes, the polarization will fluctuate between $S_N - S_F$ and $S_N + S_F$. When $q_1, q_2 \leq 0.001$ or $q_1, q_2 \geq 0.35$, the amplitude S_F becomes unimportant and the nominal spin S_N is nearly 1. Thus, these two resonances combined may be considered as spin transparent. Alternatively, when $0.001 < q_1$ and $q_2 < 0.35$, the fluctuation becomes very important.

The peak positions of the spin $S = S_N + S_F$ are located at

$$\frac{\kappa_2^2 - \kappa_1^2}{2\alpha} = (2m + 1)\pi + \mu_2 - \mu_1, \qquad m = 0, 1, 2, \ldots, \tag{42}$$

or, for small spacing ($\Delta \ll \kappa_1$),

$$\Delta \simeq \frac{\alpha}{\kappa_1} [(2m + 1) + \mu_2 - \mu_1], \qquad m = 0, 1, 2, \tag{43}$$

Thus, we expect an equal spacing for the fluctuation pattern of these two isolated resonances (see the discussion in Section 4). These highly oscillatory structures will be modulated by the slower oscillatory structure of the remaining phase in Eq. (32), i.e.,

$$f_{\text{slow}} = q_2 \ln [\tfrac{1}{2}\alpha(\theta_M - \theta_2)^2] - q_1 \ln [\tfrac{1}{2}\alpha(\theta_M - \theta_1)^2]. \tag{44}$$

The slow phase f_{slow} is, in fact, independent of θ_M, provided that Eq. (30) holds and the full spin transfer matrix is used. When the asymptotic expansion is applied, the dependence on θ_M in Eq. (44) appears. Appendix A shows the condition for which the slow phase can be neglected.
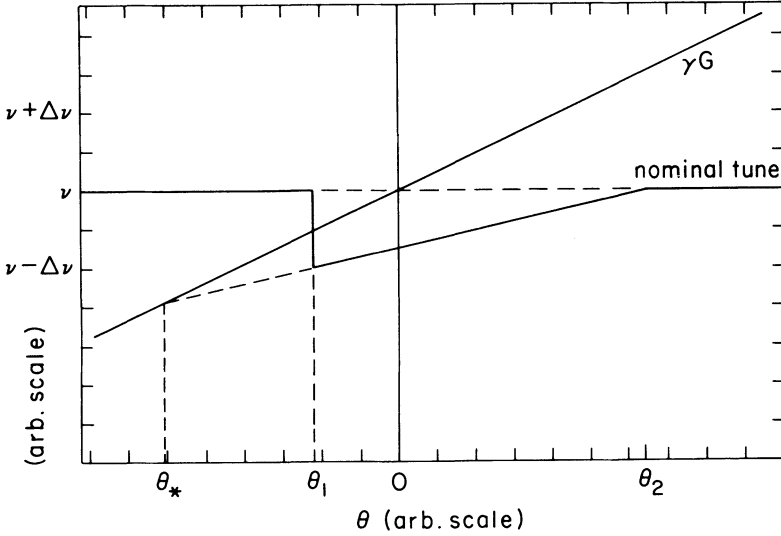
FIGURE 2 Schematic representation of resonance jumping; θ_1 is the quadrupole firing time. At $\theta = \theta_2$ the tune of the machine returns to its nominal value. θ_* is the reference crossing point between the γG and the shifting time.

3.2. Resonance Jumping

The effect of intrinsic resonances, with strengths $0.001 < q < 0.35$, can be minimized by shifting the tune during passage through resonance.[4,6] Using the spin transfer matrix developed previously, we shall now examine resonance jumping. Figure 2 shows schematically the tune shift at $\theta = \theta_1$, where the nominal resonance tune is decreased suddenly by Δv and then returns to its nominal value at $\theta = \theta_2$ after a decay time of Δt. Figure 2 also shows γG, which is also a function of θ. The slope of the resonance tune (assumed linear) between θ_1 and θ_2 is

$$\alpha_v = \frac{\Delta v}{\theta_2 - \theta_1}.$$

The resonance in this case is given by

$$\zeta(\theta) = \varepsilon e^{-i\chi(\theta)}, \tag{45}$$

where

$$\chi(\theta) = \begin{cases} v\theta + \frac{1}{2}\alpha_v(\theta^2 - 2\theta\theta_2), & \theta_1 < \theta < \theta_2 \\ v\theta, & \text{otherwise.} \end{cases}$$

Applying the matrix formulation, we obtain the spinor wave function after the resonance jump as

$$\Phi(\theta_f) = T(\theta_f, \theta_2, \theta_1, \theta_{\text{inj}})\Phi(\theta_{\text{inj}}), \tag{46}$$

where θ_f and θ_{inj} are the final and initial injection angles, respectively, and

$$T(\theta_f, \theta_2, \theta_1, \theta_{\mathrm{inj}}) = T(\theta_f)T^{-1}(\theta_2)T_t(\theta_2)T_t^{-1}(\theta_{t1})T(\theta_1)T^{-1}(\theta_{\mathrm{inj}}). \qquad (47)$$

The matrix T_t is the same as that of Eq. (18), with the following substitutions:

$$\theta \to \theta_t = \theta - \theta_*,$$

$$\varepsilon \to \varepsilon_t = \varepsilon \cdot \exp\left[-i\alpha_v^2\theta_2^2/2(\alpha - \alpha_v)\right],$$

$$q \to q_t = q \cdot \alpha/(\alpha - \alpha_v),$$

$$\alpha \to \alpha_t = \alpha - \alpha_v,$$

and

$$\theta_{t2} = \theta_2 - \theta_*,$$

where

$$\theta_{t1} = \theta_1 - \theta_*,$$

$$\theta_* = -\alpha_v\theta_2/(\alpha - \alpha_v).$$

θ_* is the point of crossing between γG and the shifted tune. The physical picture of Eq. (40) is clear in that the spinor wave function propagates from θ_{inj} to θ_1, then, during the tune shift, from θ_1 to θ_1, and finally to θ_f at final energy. The wave-function-matching procedure is realized through matrix products.

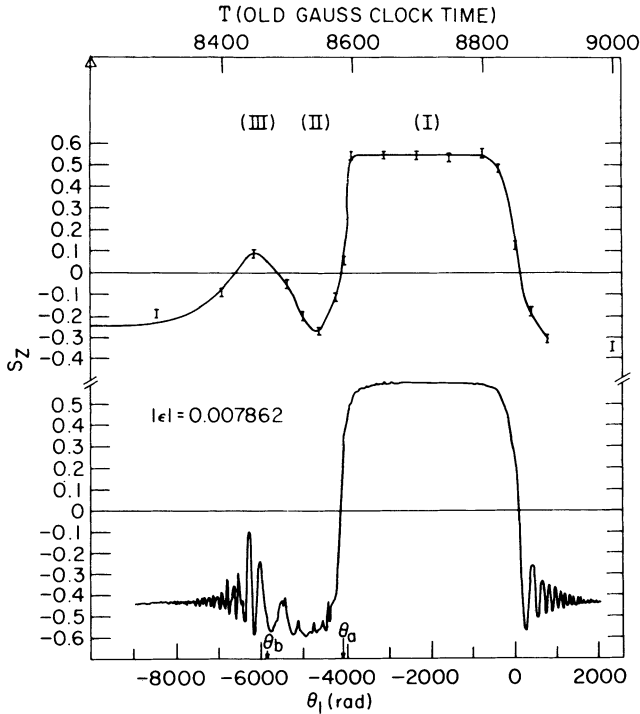Figure 3 illustrates the polarization obtained as a function of θ_1 or the

FIGURE 3   (Upper plot) Experimental polarization as a function of the quadrupole firing time (old Gauss clock or θ_1), as obtained by the AGS Data Group.[17] (Lower plot) Theoretical calculation of a simple resonance jumping model, with initial polarization of 60%. The following parameters for resonance jumping of $\gamma G = v$ are used: $\Delta v = 0.2$, $\Delta t = 2.5$ ms, $\varepsilon = -0.007862 - i0.00004$.
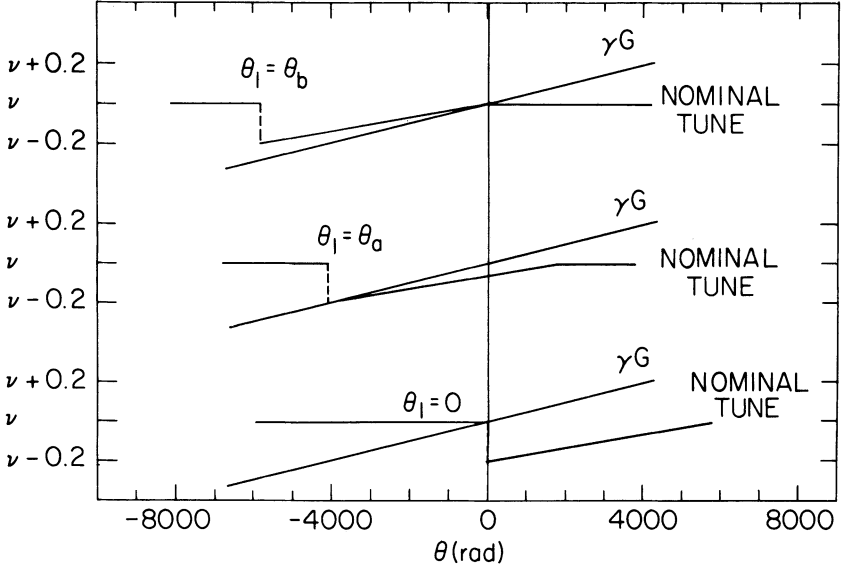
FIGURE 4   Representation of simple tune jump model for the boundaries of regions I, II, and III in Fig. 3.

resonance-jump firing time. The upper part shows the experimental results from the AGS,[16] and the calculation is shown in the lower part.[17] We observe that there are three distinct regions in this figure (marked I, II, and III). Region I is characterized by a flat plateau of negligible depolarization. Here the resonance is jumped successfully. Region II features a spin-flip. This is because the effective acceleration rate of the particle through the resonance is $\alpha - \alpha_\nu$, which is much smaller than α. Thus, the dimensionless resonance strength $\pi |\varepsilon|^2/2(\alpha - \alpha_\nu)$ is much larger. Region III appears to have interesting side-peaking.

   These three regions can be separated by three characteristic "times," 0, θ_a, and θ_b, indicated on Fig. 3. Figure 4 shows the schematic quadrupole firing sequence for $\theta_1 = \theta_a$, $\theta_1 = \theta_b$, and $\theta_1 = 0$, respectively. We see that region I corresponds to the firing time $\theta_a \leq \theta_1 \leq 0$, and region II corresponds to $\theta_b \leq \theta_1 \leq \theta_a$, where the effective acceleration rate is $\alpha - \alpha_\nu$. From Fig. 4, we find easily that

$$|\theta_a| = \Delta\nu/\alpha,$$

$$|\theta_a - \theta_b| = \Delta\nu\left(\frac{1}{\alpha_\nu} - \frac{1}{\alpha}\right).$$

Thus, the width of the spin-flip region will be smaller for smaller $\alpha - \alpha_\nu$.

4. NUMERICAL SOLUTION OF THE SPIN EQUATION

When two or more depolarizing spin resonances are close together such that there is an overlapping region where they are both important, the spin transfer matrix

method cannot be applied directly. In this case there is no known solution available at present. To study the physics of overlapping resonances, we resort to solving the classical spin equations [Eq. (2)] numerically.[1,5,6,18] It is sometimes advantageous to transform from the lab frame to the center-of-precession frame, i.e.,

$$\tilde{S}_\pm = e^{\mp i \int \kappa(\theta) d\theta} S_\pm,$$

$$\tilde{S}_3 = S_3. \tag{48}$$

Equation (2) then becomes

$$\frac{d}{d\theta} \tilde{S}_+ = i\zeta^* e^{-i\int\kappa(\theta)d\theta}\tilde{S}_3,$$

$$\frac{d}{d\theta} \tilde{S}_- = -i\zeta e^{i\int\kappa(\theta)d\theta}\tilde{S}_3, \tag{49}$$

$$\frac{d}{d\theta} \tilde{S}_3 = i(\zeta e^{i\int\kappa(\theta)d\theta}\tilde{S}_+ - \zeta^* e^{-i\int\kappa(\theta)d\theta}\tilde{S}_-).$$

Note that the resonance condition corresponds to the stationary phase in Eq. (49). The coherent contribution is the main source of depolarization.

To simplify the calculation, we consider only two resonances. The interference effect is maximized with two resonances of equal strength, i.e.,

$$\zeta(\theta) = \varepsilon_1 e^{-i\kappa_1\theta} + \varepsilon_2 e^{-i\kappa_2\theta}$$

$$= 2|\varepsilon| e^{-i(\kappa_0\theta - \phi_0)} \cos\left(\frac{\Delta\theta}{2} + \frac{\phi_1 - \phi_2}{2}\right), \tag{50}$$

where κ_0 and ϕ_0 are the average frequency and average phase of two resonances, i.e.,

$$\kappa_0 = \tfrac{1}{2}(\kappa_1 + \kappa_2),$$

$$\phi_0 = \tfrac{1}{2}(\phi_1 + \phi_2), \tag{51}$$

with $\phi_1 = \arg(\varepsilon_1)$ and $\phi_2 = \arg(\varepsilon_2)$. The parameter $\Delta = \kappa_2 - \kappa_1$ is the spacing between two resonances.

The task is to solve either Eq. (2) or Eq. (49) numerically. This is a nontrivial problem due to the highly oscillatory kernel.[7] Because of the necessity for long-term spin tracking, double precision is absolutely essential in the numerical calculation.

Results of the numerical calculation are shown in Fig. 5, where the polarization of protons at 2.41 GeV/c (or $\gamma G = 4.605$) passing through two resonances at $\kappa_1 = 3.2$ and $\kappa_2 = 3.2 + \Delta$ is plotted versus the spacing parameter Δ. The lower part of the figure corresponds to $\varepsilon = \varepsilon_1 = \varepsilon_2 = 0.05$ [Im $(\varepsilon) = 0$], which are very strong resonances. The upper part corresponds to $\varepsilon = \varepsilon_1 = \varepsilon_2 = 0.0023$, where the coherent contributions of two resonances will give zero polarization (this can be seen clearly at very small Δ in Fig. 1). The constant acceleration rate $\alpha = 4.86 \times 10^{-5}$ for the AGS is assumed for this calculation. There are no realistic double resonances at these energies in the AGS. This was chosen to save computer time. The particles, at injection energy 200 MeV, will make 7957 turns
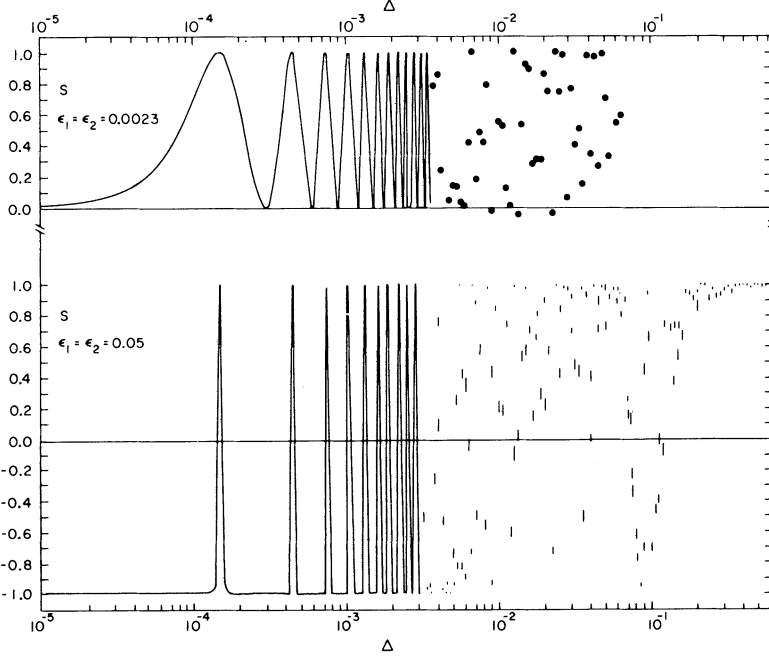
FIGURE 5 Spin polarization S of particles passing through dual spin resonances of equal strength as functions of Δ, the spacing between resonances. The upper part of the figure corresponds to the intermediate strength $\varepsilon = 0.0023$, and the lower part of the figure corresponds to a strong resonance with $\varepsilon = 0.05$. Note the regular oscillatory pattern at small Δ. The chaos of S for $\Gamma > 0.01$ in the $\varepsilon = 0.0023$ case turns out to be an orderly oscillation, which will continue to oscillate forever as Δ increases.

or 50,000 radians to reach 2.41 GeV/c. Each point in Fig. 5 takes about 30–50 CPU minutes on a VAX 11/780.

Note that the spin polarization in Fig. 5 has a very regular oscillatory behavior at small $\Delta < 0.005$. At large Δ, the polarization of particles passing through these two large resonances becomes unity. On the other hand, the polarization of particles passing through two intermediate-strength resonances fluctuates continuously and *appears* randomly distributed. The spin for large separation can be understood analytically in the next section by using the spin transfer matrix.[2] We shall address the regular oscillatory pattern at small Δ here.

When two or more resonances are within the asymptotic region[2] of each other, we call them overlapping resonances. To understand the regular oscillatory pattern of overlapping resonances in Fig. 5 for small Δ, we can rearrange Eq. (50) into a single resonance with an effective strength ε_{eff}, where

$$\varepsilon_{\text{eff}} = 2\,|\varepsilon|\,e^{i\phi_0}\cos\left[\frac{\Delta\theta}{2} + \tfrac{1}{2}(\phi_2 - \phi_1)\right]. \tag{52}$$

Since the phase of two resonances ϕ_1, ϕ_2 does not depend on θ and only shifts the peak position of ε_{eff}, we assume $\phi_1 = \phi_2 = 0$ in the calculation. For a particle

passing through the effective resonance κ_0 at $\theta = \theta_0$, we have

$$G\gamma(\theta_0) = \kappa_0. \tag{53}$$

The effective single resonance strength becomes

$$\varepsilon_{eff} = 2 |\varepsilon| \cos \left[\tfrac{1}{2} \Delta \theta_0 + \tfrac{1}{2} \Delta (\theta - \theta_0) \right]. \tag{54a}$$

In the region $|\theta - \theta_0| < \theta_A$ [see Eqs. (26)], where the particle is influenced by the resonance, the factor $\Delta(\theta - \theta_0)$ in Eq. (54a) is negligible because

$$|\tfrac{1}{2} \Delta (\theta - \theta_0)| \le |\tfrac{1}{2} \Delta \theta_A| \ll 1$$

for overlapping resonances. Therefore, the effective single resonance strength becomes

$$\varepsilon_{eff} = 2 |\varepsilon| \cos (\tfrac{1}{2} \Delta \theta_0). \tag{54b}$$

which is independent of θ. The polarization is easily found to be

$$S(\Delta) = 2 \exp \left(- \frac{\pi |\varepsilon_{eff}|^2}{2\alpha} \right) - 1$$

$$= 2 \exp \left[- \frac{2\pi |\varepsilon|^2}{\alpha} \cos^2 (\tfrac{1}{2} \Delta \theta_0) \right] - 1. \tag{55}$$

Equation (55) indicates that when

$$\Delta \theta_0 = (2m + 1)\pi, \qquad m = 1, 2, 3, \ldots \tag{56}$$

or $\Delta(\kappa - \kappa_{inj}) = (2m + 1)\pi\alpha$, then $S(\Delta)$ is peaked at a maximum value of 1. This regular oscillatory behavior is clearly seen in Fig. 5 for $\Delta < 0.005$. The equal spacing is obscured by the logarithmic scale of the abscissa.

We have treated two equal-strength resonances here. Resonances with unequal strength can be handled in a similar way. In this latter case, the cancellation of two resonances will not be exact, and the final spin is given by Eq. (55) with

$$|\varepsilon_{eff}|^2 = |\varepsilon_1|^2 + |\varepsilon_2|^2 + 2 |\varepsilon_1 \varepsilon_2| \cos (\Delta \theta_0 + \phi_2 - \phi_1),$$

where ϕ_1 and ϕ_2 are $\arg (\varepsilon_1)$ and $\arg (\varepsilon_2)$, respectively. The spin fluctuates between

$$S_{min} = 2e^{-\pi(|\varepsilon_1| + |\varepsilon_2|)^2/2\alpha} - 1 \tag{57a}$$

and

$$S_{max} = 2e^{-\pi(|\varepsilon_1| - |\varepsilon_2|)^2/2\alpha} - 1 \tag{57b}$$

with the same oscillatory frequency as that of Eq. (56). For more than two resonances, the essential picture remains the same, with some complications.

When $\Delta > 0.005$, the polarization begins to deviate from the results given by Eq. (55). Also, the actual fluctuating behavior cannot be ascertained in this region due to logarithmic compression. This fluctuating trend continues for the case $\varepsilon = 0.0023$, as Δ increases, whereas the amplitude of fluctuation vanishes for $|\varepsilon| = 0.05$ at $\Delta \geq 0.2$. For large Δ, these two resonances can be considered as nonoverlapping.

As an example, Fig. 5 shows our result for $\varepsilon_1 = \varepsilon_2 = 0.0023$ and $\alpha = 4.86 \times$
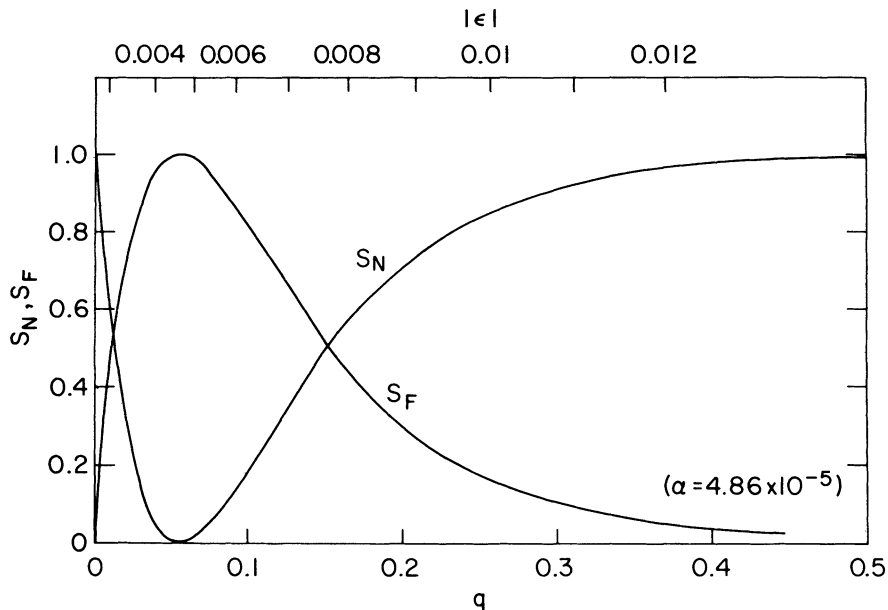
FIGURE 6 Plots of S_N and S_F versus q, for dual isolated resonances of equal strength. The coordinate scale ε corresponds to the nominal acceleration rate $\alpha = 4.86 \times 10^{-5}$ of the AGS.

10^{-5}. We have $q_1 = q_2 = 0.0136$. Thus,

$$S_{FS}(q_1) = S_{FS}(q_2) = 0.686,$$

$$S_N = 0 \cdot 470,$$

$$S_F = 0.530.$$

Thus, the total spin [Eq. (36)] would fluctuate from 1 to -0.06 at a spacing of 9.5×10^{-5}. This highly oscillatory pattern with such a small width is impossible to observe (it cannot even be plotted in Fig. 5). In fact, the tune spread of the machine would average over these fluctuations and give the final spin as the nominal value.

Figure 6 plots $S_N(q, q)$ and $S_F(q, q)$ from Eqs. (37) and (38) vs the dimensionless strength parameter q for two resonances with equal strength. It is observed easily that a large-amplitude fluctuation corresponds to a very small nominal spin polarization.

5. TUNE SPREAD AVERAGING

5.1. Overlapping Resonances

The tune spread of a machine is normally much larger than the width of the fluctuation due to the interference of two resonances; therefore, we are not able to observe the fluctuations discussed in Sections 3 and 4. Tune spread averaging is necessary to compare the experimental results with that of the theoretical calculation.

To simplify the computation, we assume that the tune of the machine has a uniform distribution, with width 2σ, around the nominal tune ν_0. Besides, each individual particle in the beam may have a different tune than its neighboring particle. These effects are lumped into a distribution function

$$P(\Delta - \Delta_0) = \begin{cases} 1/2\sigma & |\Delta - \Delta_0| < \sigma \\ 0 & \text{elsewhere,} \end{cases} \tag{58}$$

where a uniform distribution is chosen for simplicity. In the following, we shall discuss the tune averaging of two overlapping equal resonances.

The polarization due to overlapping resonances with spacing Δ_0 can then be written as

$$\langle S \rangle = \int S(\Delta) P(\Delta - \Delta_0)\, d\Delta$$

$$= 2 \int \exp\left[-16\pi q \cos^2\left(\tfrac{1}{2}\Delta\theta_0\right)\right] P(\Delta - \Delta_0)\, d\Delta - 1, \tag{59}$$

where Eq. (55) has been used. Since $\sigma \sim 10^{-3}$ is much larger than the width of fluctuation $(\sim 10^{-4})$ and the integrand in Eq. (59) is periodic, the average spin $\langle S \rangle$ becomes

$$\langle S \rangle = 2e^{-8\pi q}\frac{1}{\pi}\int_0^\pi e^{-8\pi q \cos(x)}\, dx - 1$$

$$= 2e^{-8\pi q}I_0(8\pi q) - 1, \tag{60}$$

where I_0 is the Bessel function of the second kind, order zero.[11]

Figure 7 shows the average spin $\langle S \rangle$ vs q of Eq. (60). It is interesting to note that $\langle S \rangle \simeq S_N$ of Eq. (37) at small q, i.e., $\langle S \rangle - S_N = O((8\pi q)^3)$. At large q, we
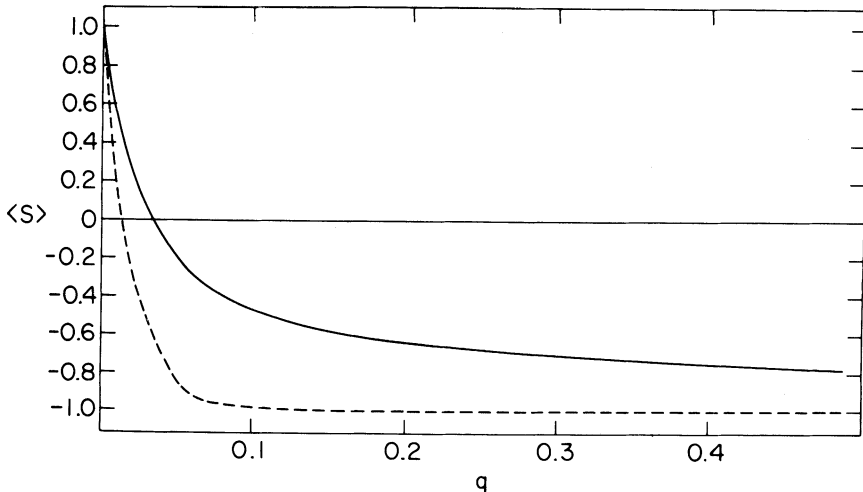

FIGURE 7   Plot of the average spin $\langle S \rangle$ as a function of q for dual overlapping resonances of equal strength (solid line). The Froissart–Stora formula for an equivalent single resonance with twice the strength is also shown (dashed curve).

have then

$$\langle S \rangle_{8\pi q \gg 1} \rightarrow -1 + \frac{1}{2\pi \sqrt{q}}. \tag{61}$$

Thus *strong* overlapping resonances are not particularly harmful to the spin polarization of the particles. The remaining amount of polarization for $q = 0.35$ is approximately 73%. This is evident from the lower part of Fig. 1, where we observe that the fluctuation width becomes extremely narrow for strong resonances.

5.2. Tune Averaging for Isolated Resonance

Tune averaging for an isolated resonance is relatively simple because of the simplicity of Eq. (36). The average spin becomes the nominal value, i.e.,

$$\langle S \rangle = S_N,$$

and the standard deviation becomes

$$\sigma_s = \frac{1}{\sqrt{2}} S_F.$$

The only way that these two resonances might not depolarize the spin is if both of them are either strong ($q > 0.35$) or weak ($q < 0.001$). Separate corrections should be possible because they are isolated.

6. CONCLUSION

We have reformulated the acceleration of polarized protons through depolarizing resonances in terms of products of spin transfer matrices. For a single resonance, the spin transfer matrix gives the Froissart–Stora formula. For many nonoverlapping resonances, the spin transfer matrix method can easily be used to calculate the polarization of particles passing through these resonances. We have discussed the effect of the phase of precession on final polarization for two resonances. It was found that intermediate resonance strengths ($0.001 \leq q \leq 0.35$) must be handled carefully in order to get a high degree of polarization. Intrinsic resonances between 0.001 and 0.35 should be jumped by shifting the tune appropriately. The matrix formulation was applied to resonance jumping, giving good agreement with experimental data.

   These applications are illustrative examples of the method of the spin transfer matrix. The method offers a clear physical picture for the acceleration of particles through depolarizing resonances.

   We have also studied numerically the acceleration of polarized protons through two resonances. We found, first, that when two resonances are overlapping the final spin will fluctuate at a regular spacing. For stronger resonances, the fluctuation will be correspondingly sharper. The range of fluctuation will be

between S_{min} and S_{max} of Eqs. (57a) and (57b), respectively. Since the spacing of these fluctuations is very small, tune spread averaging is very important. Because of the sharp spike in the polarization passing through two strong resonances (see Fig. 5), the tune average does not substantially depolarize the spins of the particles. However, when the resonances are weak, correction procedures have to be used to get a respectable final polarization. Because of the finite tune spread of the machine, the interference effect between two resonances is not effective for the cancellation of two resonances.

We also found that when two resonances are isolated the spin transfer matrix method can be applied to understand the physics of the interference of these resonances. For strong resonances ($q > 0.35$) or weak resonances ($q < 0.001$), the phase of precession between the two resonances is not important. For resonances with intermediate strength ($0.001 < q < 0.35$), the phase becomes very important. The final spin will fluctuate around the nominal values of S_N with fluctuation amplitude S_F; these values are given by Eqs. (37) and (38), respectively. S_N becomes the final spin of the particles when the tune averaging procedure is considered.

Finally, we should mention that we solved two spin resonance problems numerically by using a double-precision version of a differential equation solver with the Adams method.[9] We found that the spins of the particles can be tracked successfully. It takes approximately 30–50 CPU minutes in the VAX 11/780 machine to track the spin 10^4 turns, depending on the strength of the depolarizing resonances. The method can also be used to study resonance jumping with a nonlinear time decay constant.

ACKNOWLEDGMENT

REFERENCES

1. G. M. Bunce, Ed., *High Energy Spin Physics—1982*, AIP Conference Proceedings No. 95 (Am. Inst. Phys., New York, 1983).
2. V. Bargmann, L. Michel, and V. L. Telegdi, *Phys. Rev. Lett.* **2**, 439 (1959).
3. M. Froissart and R. Stora, *Nucl. Instrum. Methods* **7**, 297 (1960).
4. E. D. Courant and R. D. Ruth, *The Acceleration of Polarized Protons in Circular Accelerators*, Brookhaven National Laboratory report BNL-51270 (1980).
5. B. W. Montague, *Particle Accelerators* **11**, 219 (1981).
6. T. Khoe, R. L. Kustom, R. L. Martin, E. F. Parker, C. W. Potts, A. D. Krisch, J. B. Roberts, and J. R. O'Fallon, *Particle Accelerators* **6**, 213 (1975).
7. E. Grorud, J.-L. Laclare, G. Leleux, A. Nakach, and A. Ropert, in Ref. 1, p. 407.
8. L. G. Ratner, in Ref. 1, p. 412.
9. S. Tepikian, S. Y. Lee, and E. D. Courant, Brookhaven National Laboratory report BNL-36264.
10. L. F. Shampine and H. A. Watts, Sandia National Laboratories report SAND79-2374 (1979). L. F. Shampine and M. K. Gordon, program DEABM, May 1980, revised Oct. 1981, Sandia National Laboratories.

11. M. Abramowitz, and I. A. Stegun, Eds., *Handbook of Mathematical Functions* (Dover, New York, 1965).
12. A. Erdélyi et al., *Higher Transcendental Functions*, Vol. 1 (McGraw-Hill, New York, 1953), Chap. 6.
13. S. Y. Lee and N. Takigawa, *Nucl. Phys.* **A308**, 189 (1978).
14. E. D. Courant and H. S. Snyder, *Ann. Phys.* **3**, 1 (1958).
15. R. D. Ruth, in Ref, 1. p. 378.
16. L. Ratner, and AGS Data Group, private communication.
17. S. Y. Lee, S. Tepikian, and E. D. Courant, AGS Tech. Note AGS-207.
18. S. Y. Lee, S. Tepikian, and E. D. Courant, Brookhaven National Laboratory report BNL-36265.

APPENDIX A

Spin Precussion in Circular Accelerators

Following Courant and Ruth,[4] we define the Frenet–Serret curvilinear coordinates as

s = distance along the reference orbit,

$\rho(s)$ = local radius of curvature of the reference orbit,

$\mathbf{r}_0(s)$ = the reference orbit,

$\hat{s} = d\mathbf{r}_0/ds$ = the unit tangent reactor,

$\hat{x}$ = unit vector in the orbit plane perpendicular to $\hat{s}$,

$\hat{y} = \hat{z} = \hat{x} \times \hat{s}$.

We also have the following relations:

$$\frac{d\hat{x}}{ds} = \frac{\hat{s}}{\rho}, \qquad \frac{d\hat{s}}{ds} = -\frac{\hat{x}}{\rho}, \qquad \frac{d\hat{y}}{ds} = 0. \tag{A-1}$$

An arbitrary point near the reference orbit is given by

$$\mathbf{r} = \mathbf{r}_0(s) + x\hat{x} + y\hat{y}. \tag{A-2}$$

The velocity of a particle is

$$\mathbf{V} = \frac{d\mathbf{r}}{dt} = \frac{ds}{dt}\frac{d\mathbf{r}}{ds} = \frac{ds}{dt}\left[x'\hat{x} + \left(1 + \frac{x}{\rho}\right)\hat{s} + y'y\right], \tag{A-3}$$

where a prime denotes differentiation by s. Keeping terms linear in ds/dt, x, z, and their derivatives, we find that

$$V = |\mathbf{V}| = \frac{ds}{dt}\left(1 + \frac{x}{\rho}\right), \tag{A-4}$$

or

$$\mathbf{V} = V(x'\hat{x} + \hat{s} + y'\hat{y}), \tag{A-5}$$

$$\mathbf{V}' = V\left[\left(x'' - \frac{1}{\rho}\right)\hat{x} + \frac{x'}{\rho}\hat{s} + y''\hat{y}\right].$$

The transverse magnetic field becomes

$$\mathbf{B} = \frac{1}{V^2}(\mathbf{V} \times \mathbf{B}) \times \mathbf{V} = \frac{\gamma mc}{eV^2}\left(\frac{d\mathbf{V}}{dt}\right) \times \mathbf{V}$$

$$= B\rho\left(1 - \frac{x}{\rho}\right)\left[-y''\hat{x} + \left(x'' - \frac{1}{\rho}\right)\hat{y} + \frac{y'}{\rho}\hat{s}\right], \quad \text{(A-6)}$$

where $B\rho = \gamma mvc/e$ is the magnetic rigidity of the particle, and the Lorentz force is used in deriving the above equation.

The next task is to obtain $B_\parallel$ in terms of particle coordinates. We assume that the longitudinal field B_s on the reference orbit is zero. Applying Maxwell's equations, we have

$$\frac{\partial B_s}{\partial y} = \frac{\partial B_y}{\partial s} = -B\rho\frac{d}{ds}\left(\frac{1}{\rho}\right), \quad \text{(A-7)}$$

where the guide field $B_y = -(B\rho)/\rho$ is used. Thus,

$$B_s = -(B\rho)y\frac{d}{ds}\left(\frac{1}{\rho}\right). \quad \text{(A-8)}$$

To first order,

$$\mathbf{B}_\parallel = B_s\hat{s} + y'B_y\hat{s} = -\left[B\rho y\left(\frac{1}{\rho}\right)' + (B\rho)\frac{y'}{\rho}\right]\hat{s}$$

$$= -B\rho\left(\frac{y}{\rho}\right)'\hat{s}. \quad \text{(A-9)}$$

Substituting Eqs. (A-6) and (A-9) into Eq. (1), we obtain

$$\frac{d\mathbf{S}}{ds} = \mathbf{S} \times \mathbf{F}, \quad \text{(A-10)}$$

where

$$\mathbf{S} = S_1\hat{x} + S_2\hat{s} + S_3\hat{y}$$
$$\mathbf{F} = F_1\hat{x} + F_2\hat{s} + F_2\hat{Y}$$
$$= -(1 + \gamma G)y''\hat{x} + \left[(1 + \gamma G)\frac{y'}{\rho} - (1 + G)\left(\frac{y}{\rho}\right)'\right]\hat{s} + (1 + \gamma G)\left(x'' - \frac{1}{\rho}\right)\hat{y}. \quad \text{(A-11)}$$

Making a coordinate transformation, $\theta = \int_0^s ds/\rho$, and using Eq. (A-1), we obtain

$$\frac{dS_1}{d\theta} = -\kappa S_2 - rS_3,$$

$$\frac{dS_2}{d\theta} = \kappa S_1 - tS_3, \quad \text{(A-12)}$$

$$\frac{dS_3}{d\theta} = rS_1 + tS_3,$$

where

$$\kappa = \gamma G - (1 + \gamma G)\rho \simeq \gamma G,$$

$$r = (1 + \gamma G)y' - \rho(1 + G)\left(\frac{y}{\rho}\right)', \qquad \text{(A-13)}$$

$$t = (1 + \gamma G)\rho y'',$$

APPENDIX B

Asymptotic Expansion of Confluent Hypergeometric Functions

Equations (18) show that the spinor wave function for a single resonance can be put in the form:

$$\Phi(\theta_f) = \begin{pmatrix} z(\theta_f) & -w(\theta_f) \\ \bar{w}(\theta_f) & \bar{z}(\theta_f) \end{pmatrix} \begin{pmatrix} z(\theta_i) & -w(\theta_i) \\ \bar{w}(\theta_i) & \bar{z}(\theta_i) \end{pmatrix}^{-1} \Phi(\theta_i), \qquad \text{(B-1)}$$

where $\Phi(\theta_i)$ is the initial two-component spinor function and $\Phi(\theta_f)$ is the resulting spinor.

The purpose of this appendix is to consider the case where θ_f and θ_i are large. This is done by considering the asymptotic expansion of confluent hypergeometric functions,[11,12]

$$M(a, b; z) \sim \frac{\Gamma(b)}{\Gamma(b - a)} e^{\pm i\pi a} z^{-a} + \frac{\Gamma(b)}{\Gamma(a)} e^z z^{a-b} + \cdots, \qquad \text{(B-2)}$$

where the $\pm$ sign corresponds to $\mathrm{Im}\,(z) \lessgtr 0$, respectively. With the asymptotic expansion in Eq. (B-2), the $z(\theta)$ and $w(\theta)$ of Eqs. (18a) and (18b) become

$$z(\theta) \sim \frac{\Gamma(\frac{1}{2})}{\Gamma(\frac{1}{2} - iq)} \exp\left(-\pi q/2\right) \exp\left[-iq \ln\left(\tfrac{1}{2}\alpha\theta^2\right)\right] + \cdots, \qquad \text{(B-3)}$$

$$w(\theta) \sim \pm \frac{i}{2}\varepsilon \sqrt{\frac{2}{\alpha}} \frac{\Gamma(\frac{3}{2})}{\Gamma(1 - iq)} \exp\left(i\pi/4\right) \exp\left(-\pi q/2\right) \exp\left[-iq \ln\left(\tfrac{1}{2}\alpha\theta^2\right)\right] + \cdots, \tag*{(B-4)}$$

where the plus sign is for $\theta > 0$ and the minus is for $\theta < 0$. With Eqs. (B-3) and (B-4), the matrix of Eq. (B-1) becomes

$$\Phi(\theta_f) = \exp\left[-iq \ln\left(\tfrac{1}{2}\alpha\theta_f^2\right)\sigma_3\right] U(q) \exp\left[iq \ln\left(\tfrac{1}{2}\alpha\theta_i^2\right)\sigma_3\right]\Phi(\theta_i), \qquad \text{(B-5)}$$

where

$$U(q) = \begin{pmatrix} e^{-2\pi q} & C(q) \\ -\bar{C}(q) & e^{-2\pi q} \end{pmatrix} \qquad \text{(B-6)}$$

with

$$C(q) = -\frac{i}{4}\varepsilon \sqrt{\frac{2}{\alpha}} \frac{\Gamma(\frac{1}{2} + iq)}{\Gamma(1 - iq)} e^{i\pi/4} e^{-\pi q}(e^{\pi q} + e^{-\pi q}).$$

The condition for the validity of the asymptotic expansion is given by

$$|\theta| \gg \theta_T,$$

where

$$\tfrac{1}{2}\alpha\theta_T^2 = q\,\frac{\cosh \pi q}{\sinh \pi q}\,. \tag{B-7}$$

Curve 1 in Fig. 1 shows q of Eq. (B-7) as a function of $\tfrac{1}{2}\alpha\theta_T^2$.

Let us now rewrite Eq. (B-5) in the laboratory frame:

$$\psi(\theta_f) = \exp\left(-\frac{i}{2}\int_0^{\theta_f}\gamma G\,d\theta\sigma_3\right)\exp\left[-iq\ln(\tfrac{1}{2}\alpha\theta_f^2)\sigma_3\right]$$

$$\cdot\, U(q)\exp\left[-iq\ln(\tfrac{1}{2}\alpha\theta_i^2)\sigma_3\right]\exp\left(\frac{1}{2}\int_0^{\theta_i}\gamma G\,d\theta\sigma_3\right)\cdot\psi(\theta_i). \tag{B-8}$$

Note here that the precession induced by the resonance can be neglected if

$$\frac{1}{2}\int_0^{\theta}\gamma G\,d\theta \gg q\ln\tfrac{1}{2}\alpha\theta^2$$

or

$$\theta \gg \theta_T,$$

where

$$q = \frac{1}{2}\frac{\tfrac{1}{2}\alpha\theta_T^2}{\ln(\tfrac{1}{2}\alpha\theta_T^2)}\,. \tag{B-9}$$

Curve 2 in Fig. 1 shows q vs $\tfrac{1}{2}\alpha\theta_T^2$ for Eq. (B-9). Note especially that the region where θ is much larger than θ_T for both curves has a special meaning, namely, that the resonance plays little role in the precession of the spin. We thus call this region the asymptotic region of the resonance, as marked in Fig. 1.